Hindawi
Shock and Vibration
Volume 2019, Article ID 4232730, 8 pages
https://doi.org/10.1155/2019/4232730

Research Article

Influence of Load Weight on Dynamic Response of Vibrating Screen

Yong-Zheng Jiang,[1] **Kuan-Fang He**,[1] **Yong-Le Dong**,[2] **Da-lian Yang**,[1] **and Wei Sun**[2]

[1]*Hunan Provincial Key Laboratory of Health Maintenance for Mechanical Equipment, Hunan University of Science and Technology, Xiangtan 411201, China*
[2]*Henan Gengli Engineering Equipment Co., Ltd., Luoyang 471132, China*

Correspondence should be addressed to Yong-Zheng Jiang; jiangyz186@126.com

Received 2 January 2019; Revised 6 March 2019; Accepted 21 March 2019; Published 11 April 2019

Academic Editor: Enrico Zappino

The dynamic response of the vibrating screen has a great impact on the screening efficiency and fatigue life of the structures. For the conventional dynamic design, the consideration of the influence of load weight on dynamic response is lacking. So, in this paper, taking a very common vibrating screen used in tunnel construction as an example, the relationship between the screen dynamic response and the load weight is studied through numerical simulations. Firstly, to make sure the accuracy of simulation, the three-dimensional finite element model of a vibration screen is strictly built to maximize consistency with the real screen, and then the simulated results are validated by experiments. Furthermore, the variation regularity of dynamic response with the load weight and excitation frequency is analyzed based on simulations. Results show the load weight has obvious influence on the modal shapes as well as the natural frequencies. There are three regions that will lead to the sudden increase of vibration acceleration: (1) the load weight variates within 0–50 kg and excitation frequency variates within 40–60 Hz; (2) the load weight variates within 10–100 kg and excitation frequency variates within 50–90 Hz; (3) the load weight variates within 80–200 kg and excitation frequency variates within 70–100 Hz. These results will provide new theoretical reference for the maintenance and further improvement in the dynamic design of the vibrating screen.

1. Introduction

The vibration screen which is an important kind of sizing classifier is widely used in various industries. The screen works by the action of the excitation which usually produces periodic alternating centrifugal force by the rotation of eccentric mass. In the working process, due to the inappropriate design of the structures and the unsuitable parameter settings, the vibrating screen is prone to underload or overload conditions, which results in bad screening effect or induces fatigue cracks and even causes serious accidents such as collapse of the whole machine [1–3]. Therefore, it is of great significance to study the response of the vibrating screen for improving the screen effect and prolonging the fatigue life of the equipment.

For the better design of the structures, a lot of studies concerned with the natural frequencies, dynamic response, and screening efficiency have been carried out recently. And, the existing research methods mainly include experiment and numerical simulation which mainly incorporates finite element method (FEM) and discrete element method (DEM) [4]. With the fast development of solution technology, FEM simulations have been widely applied for calculating the natural frequencies of the vibrating screen. Through comparison with the corresponding modal experiments, it has been proved the FEM simulation results can accurately predicted the real natural frequencies through well-accordant modeling [5, 6]. Based on FEM simulations, dynamic response characteristics of screen were widely studied, especially the influence of structure parameters on dynamic response characteristics [7], so are the dynamic responses changing regularities of vibrating screen under different forced vibration frequencies [8, 9]. Furthermore, complex particle flow-behavior and screening efficiency on

the vibrating screen were studied by simulations based on the discrete element method [10, 11]. Based on DEM, the functional relationship between screening efficiency and screen length is established, and the sensitivity of the roller screen performance to material parameters and operating variables is studied [12–14].

In general, existing literatures have studied the natural frequencies, dynamic response, and screening efficiency through experiments and numerical simulations, and the obtained results have a good guiding significance for the structure design as well as screening performance improvement. However, currently, the study on the influence of the changing weight of bulk materials on the dynamic response of screen is lacking. In actual working process, the weight of bulk materials on the sieve decreases gradually, which will lead to the variation of natural frequencies of the vibration systems, so that dynamic response of the structures will also change. This change is very likely to cause the worse of screening effect or the failure of structure strength. However, usually, conventional design calculates the dynamic parameter based only on empty or full load of the screen [15, 16], ignoring the weight change which has important influence on the vibration system. So, this paper focuses on the study of relationship among the response, load weight, and excitation frequencies to provide new theoretical reference for dynamic design of vibrating screens.

2. Motional Differential Equation

The vibration system is mainly made up of the exciter, screen, and bulk material. In the actual working process, the weight of the vibration system decreases gradually as the bulk material falls down. The motional differential equation can be written as

$$[M(t)]\{\ddot{u}(t)\} + [C]\{\dot{u}(t)\} + [K]\{u(t)\} = \{F(t)\}, \quad (1)$$

where mass matrix $[M(t)]$ varies as a function of time; $[K]$ denotes stiffness matrix; and $\{\ddot{u}(t)\}$, $\{\dot{u}(t)\}$, $\{u(t)\}$, and $\{F(t)\}$ denote the acceleration, velocity, displacement, and excitation force, respectively.

Obviously, equation (1) is a variable coefficient differential equation rather than ordinary differential equation when the time-varying of vibration mass is counted. Its characteristic equation is

$$\left|[K] - \omega^2 [M(t)]\right| = 0. \quad (2)$$

Due to the time-varying of $[M]$, the eigenvalue ω and the corresponding eigenvector A are also time-varying, and they can be expressed in the following form:

$$\begin{aligned} \omega_i &= \omega_i(t), \\ A_i &= A_i(t). \end{aligned} \quad (3)$$

According to the forced vibration theory, the screen vibration frequency and acceleration are decided together by the natural frequencies, excitation frequency, and damping ratio. Therefore, due to the change of system natural frequencies caused by the falling down of bulk material, the dynamic response of the screen will also change dramatically in the screening process.

3. FE Modeling and Experiment Verification

3.1. 3D Finite Element Modeling. In this paper, the vibrating screen used in tunnel construction is chosen for study. Figure 1(a) shows its structure which is composed mainly of a frame, a sieve, an exciter, and four support springs. The size of the screen is 1.125 meter long, 0.925 meter wide, and 0.14 meter high, and screen hole is square and the size is 0.039 meter long by 0.043 meter wide. The sieve material is stainless steel X6Cr17 with elastic modulus 2*E*5 MPa, yield strength 240 MPa, and ultimate tensile strength 430 MPa. The material of the four supporting coil springs which are mounted on the foundation is 60Si2Mn, and each spring is 120 mm long, with stiffness 50.4 N/mm.

As for the powerful modeling capability, the commercial software HYPERMEHS 13.0 edition is selected for the establishment and analysis of finite element model. For modal analysis, the key to high accuracy of simulation model depends on the similarity of the structure, mass, and stiffness between the model and the real object. Therefore, to make sure the accuracy of simulation model, the weight, shape, and structure of each component is strictly built to maximize consistency with the real screen. In the FE modeling, the plates of the frame are modeled with shell elements which represent the real plates by assigning shell thickness. The sieve which is made up of beams is modeled with beam elements which represent the real beams by assigning beam cross-section shapes. The exciter is simplified as a mass element which owns the same mass, and the four supporting coil springs are simplified as spring elements which are assigned the same stiffness. All the freedoms of the end node of the spring elements are constrained, and a sine excitation of 2000 N amplitude with frequency of 53 Hz is applied on the mass element. After the process of geometric cleaning, midsurface extraction, meshing, mesh quality control, and so on, the finished high-quality simplified finite element model with mixed element types is shown as Figure 1(b).

3.2. Modal and Harmonic Frequency Response Analysis

3.2.1. Modal Analysis. Since obtaining the natural frequencies is the basis of the dynamic response analysis, in this paper, block Lanczos method is adopted for solving the natural frequencies, the results consist of the first four natural frequencies, and modal shapes are shown in Figure 2. The first natural frequency is 25.54 Hz, and the corresponding modal shape (Figure 2(a)) is the overall warpage. This modal shape needs to be avoided as much as possible in working process because it has no help for screening but it is harmful to the structure strength. For the second, third, and fourth frequencies, the values are 52.62, 101.57, and 126.29 Hz, respectively. All these three screen modal shapes are the z direction motion which is just the needing movement type for screening.

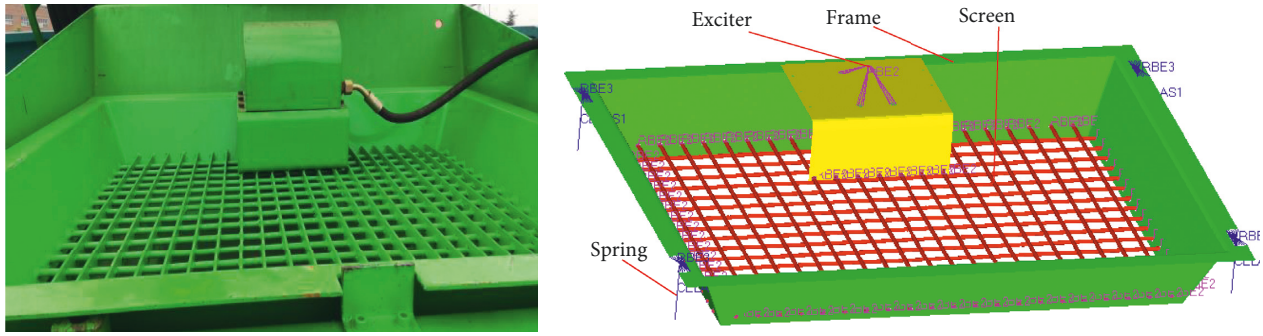

(a) (b)

Figure 1: Structure of the vibrating screen: (a) real vibrating screen; (b) finite element model.

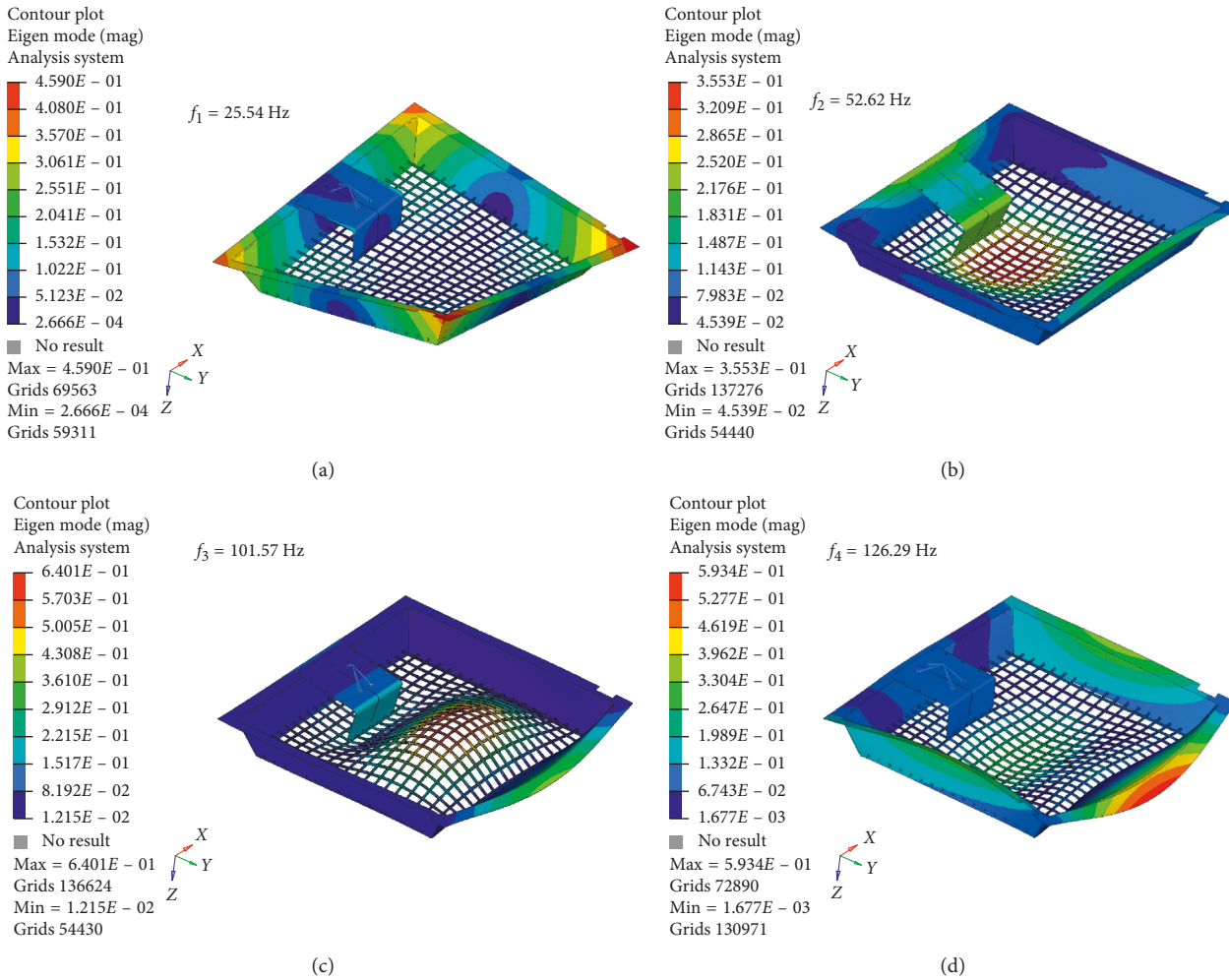

Figure 2: The first four modes of the vibrating screen: (a) the first mode; (b) the second mode; (c) the third mode; (d) the fourth mode.

3.2.2. Harmonic Frequency Response. The harmonic frequency response is scanned from 20 to 95 Hz. Simulated results show the acceleration of the screen center varies with excitation frequency dramatically. The max acceleration reaches 304 m/s^2 (Figure 3(a)), and the acceleration value is 279 m/s^2 when the exciter generates excitation force of 53 Hz. Under this work condition, the acceleration distribution of the whole structure is shown as Figure 3(b). It can be seen that the acceleration is unevenly distributed, and the maximum acceleration happens near the center of the screen. For comparison with the following test results, values at five different places are presented. They are 18 m/s^2 of x direction on the exciter, 279 m/s^2 of z direction at the center of screen, 158 m/s^2 of z direction on the frame center, 12 m/s^2 of x

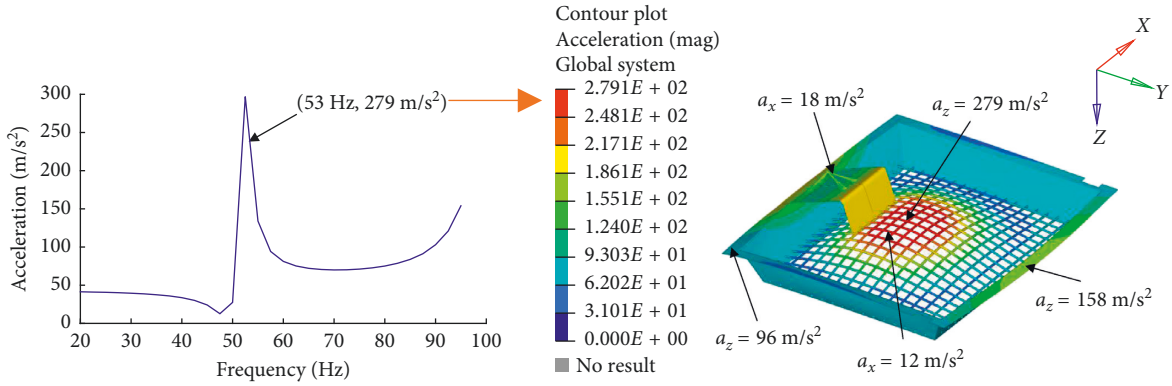

Figure 3: Dynamic frequency response: (a) acceleration variation with frequency; (b) acceleration distribution of the screen under excitation of 53 Hz.

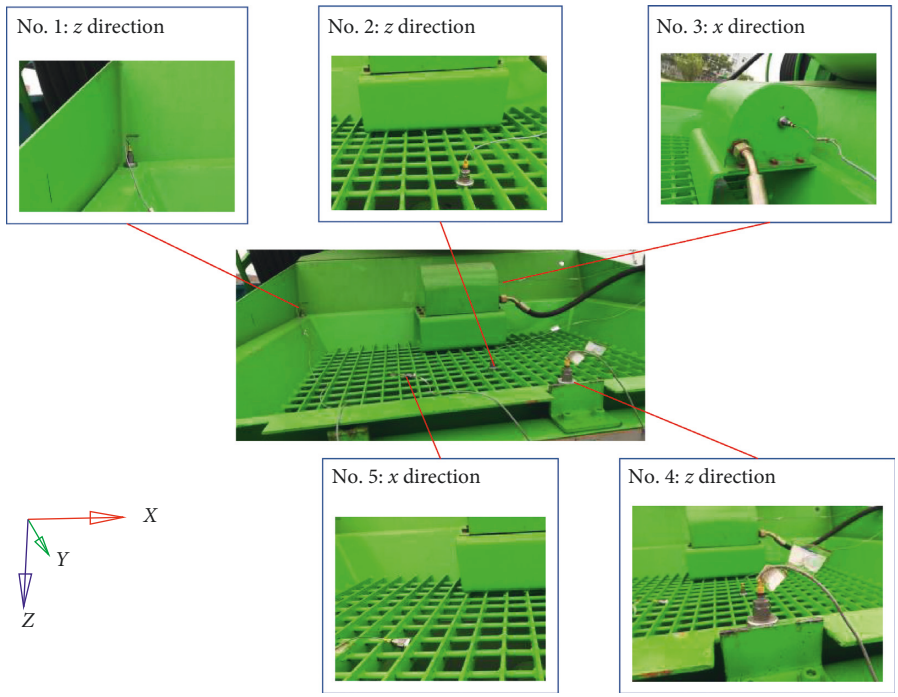

Figure 4: The positions of five accelerometers.

direction on the screen center, and 96 m/s^2 of z direction on the frame left corner, respectively.

3.3. Experiment Verification. To validate the results of the simulation model, corresponding experiments are carried out to test both the natural frequency and the accelerations of the five positions in Figure 3(b). The experiment program is as shown in Figure 4. There are totally five accelerometers mounted, respectively, at the five key positions. Sensors No. 1, No. 2, and No. 4 are mounted on the frame and screen for measuring z direction acceleration signals, while sensors No. 3 and No. 5 are mounted on the exciter and screen for measuring x direction acceleration signals. In a single test procedure, at first, the screen is in static state, after then the exciter begins to rotate at 53 Hz, so that obvious vibration occurs. After about 10 seconds, the exciter is suddenly powered off, leaving the screen vibration decaying freely until it stops completely. This test procedure is repeated two times, and the in-time signals of five sensors are shown as Figure 5. It can be seen that repeated signal is very close to the origin. For calculating the natural frequencies, the fast Fourier-transform (FFT) is applied to convert the free decay signals of No. 1 from the time domain into the frequency domain which is shown as Figure 5(b). In total, three natural frequencies can be obviously identified. They are 24.9, 52.8, and 98.8 Hz, respectively, which corresponds fairly closely with the simulated results of 25.54, 52.62, and 101.57 Hz. Further, the measured acceleration value of the five key positions are 89, 230, 14, 128, and 7.5 m/s^2, which also corresponds fairly closely with the simulated results of 96, 279, 18, 158, and 12 m/s^2.

The percentage of difference between FEM and experimental results is reported in Table 1. It can be seen that the simulated values of the three natural frequencies are very close to the experimental ones, and the error is within 3%.

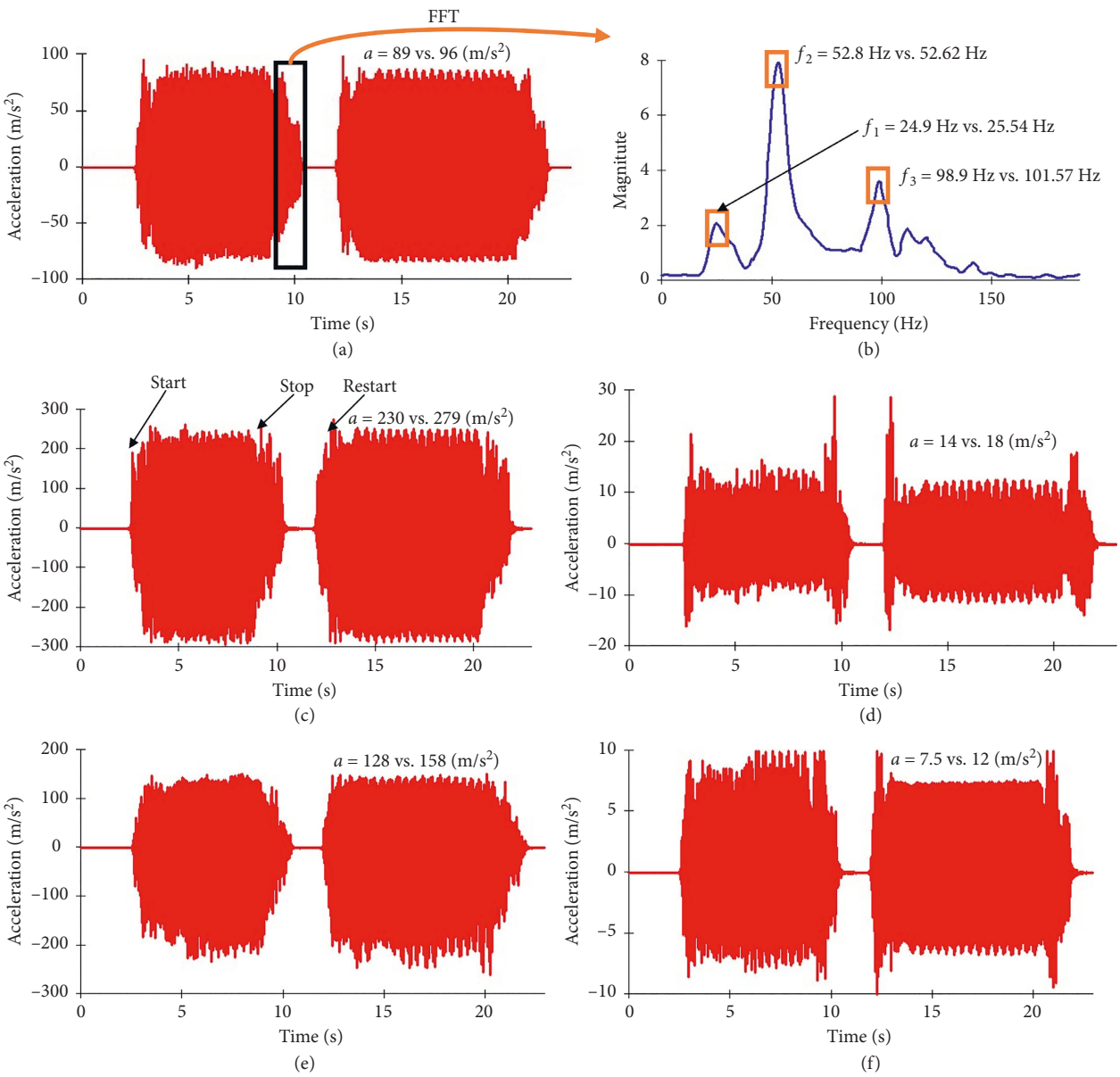

Figure 5: Experiment results: (a) signal of sensor No. 1; (b) FFT results of the free decay signal; (c) signal of sensor No. 2; (d) signal of sensor No. 3; (e) signal of sensor No. 4; (f) signal of sensor No. 5.

But for the comparison of the acceleration values at the five measured positions, the average difference of the five positions between FEM and experimental results is 17.7%. Since it is very difficult to calculate the acceleration values quantitatively, it is already very valuable to reach this precision at so many positions. Also, the acceleration distribution of the simulation is very similar to experimental results. So, based on an overall consideration, the simulation model can be regarded as high precision.

4. Relationship between the Dynamic Response and Load Weight

In actual production process, the load weight of the vibrating screen is time-varying as the bulk material falls down. So, it is important to study the changing trend of vibration response with the load weight which varies within 0–200 kg for this study.

4.1. Natural Frequency Varies with Load Weight. Variation of the first four natural frequencies with load weight is shown as Figure 6. It clearly shows that all the four natural frequencies are lowered as the weight increases. When the mass reaches 200 kg, the frequencies are reduced to 11.60, 26.55, 45.09, and 48.27 Hz, respectively. Moreover, the modal shape of the fourth frequency also changes when the mass is over 20 kg and the new shape is convex on left and concave on the right, rather than overall convex of empty load, as shown in Figure 7.

4.2. Regularity of the Dynamic Response Changing with Load Weight and Excitation Frequency. Since the load weight has

Table 1

	f_1	f_2	f_3	a_1	a_2	a_3	a_4	a_5
Experiment	24.9	52.8	98.9	89	230	14	128	7.5
FEM	25.54	52.62	101.57	96	279	18	158	12
Percentage error	2.5	0.3	2.6	7.3	17.6	22.2	19.0	37.5

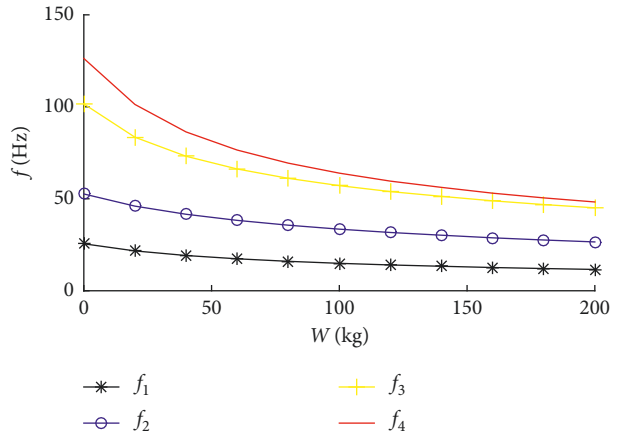

Figure 6: Variation of the first four natural frequencies with load weight.

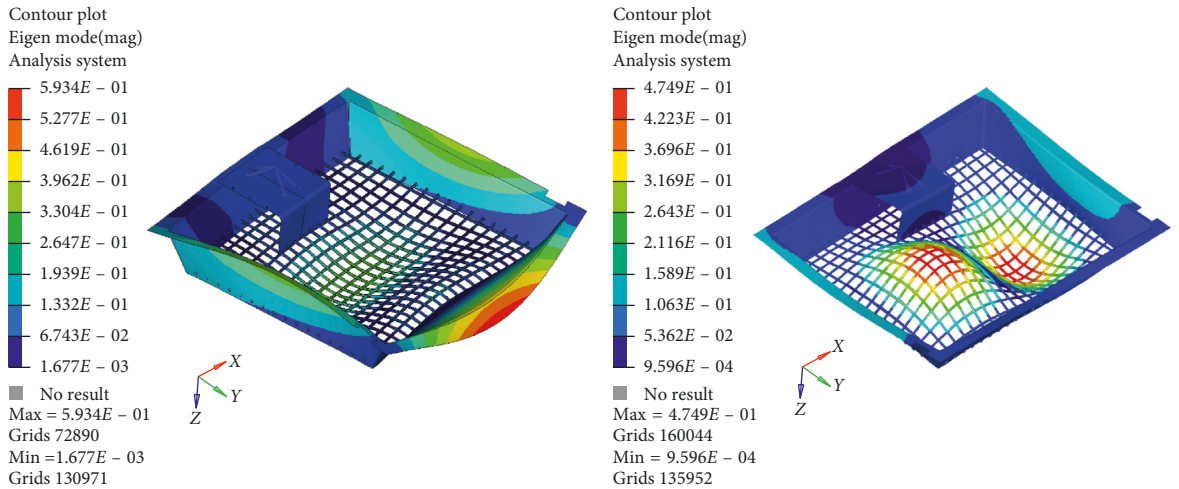

Figure 7: The fourth modal shape of (a) empty-load screen and (b) load weight over 20 kg.

significant influence on the natural frequency of the screen, the vibration response will also be different under different load weights. After many calculations, the relationship between the vibration response of the screen center, material weight, and excitation frequency is built as shown in Figure 8. It can be seen the dynamic response varies dramatically with the change of weight and excitation frequency. There are three paths that will lead to the sudden increase of vibration acceleration. They are as follows: (1) the load weight variates within 0–50 kg and excitation frequency within 40–60 Hz. In this region, the maximum acceleration reaches about 300 m/s^2, and the typical modal shape is overall concave, as shown in Figure 9(a); (2) the load weight variates within 10–100 kg and excitation frequency within 50–90 Hz. In this region, the maximum acceleration reaches about 1200 m/s^2, and the typical modal shape is double concave, as shown in Figure 9(b); (3) the load weight variates within 80–200 kg and excitation frequency within 70–100 Hz. In this region, the max acceleration reaches about 800 m/s^2, and the typical modal shape is triple concave, as shown in Figure 9(c).

5. Conclusions

This paper aims to study the relationship between the vibration response, load weight, and excitation frequency

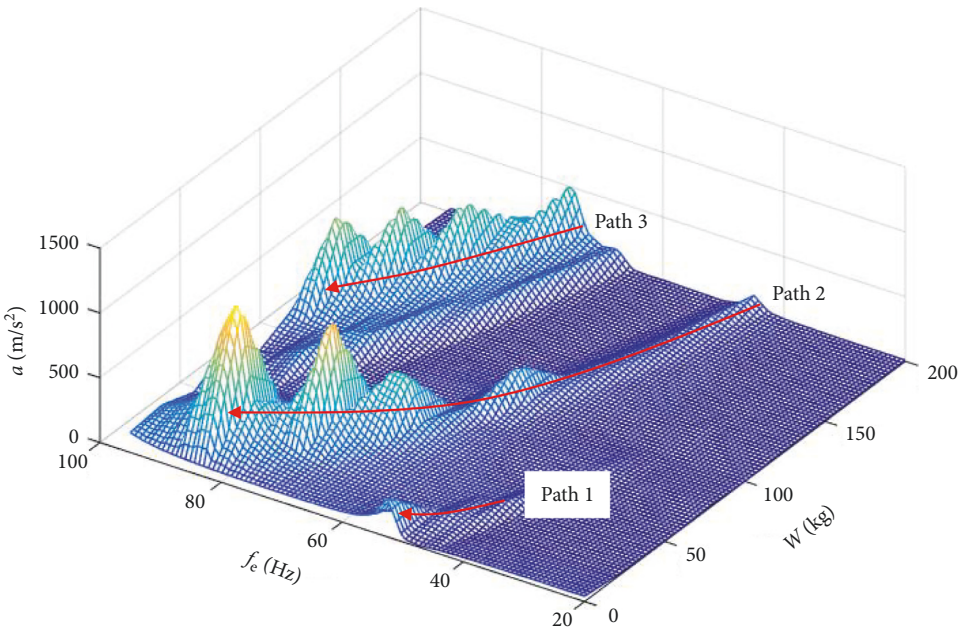

Figure 8: Changing regularity of the dynamic response with the load weight and excitation frequency.

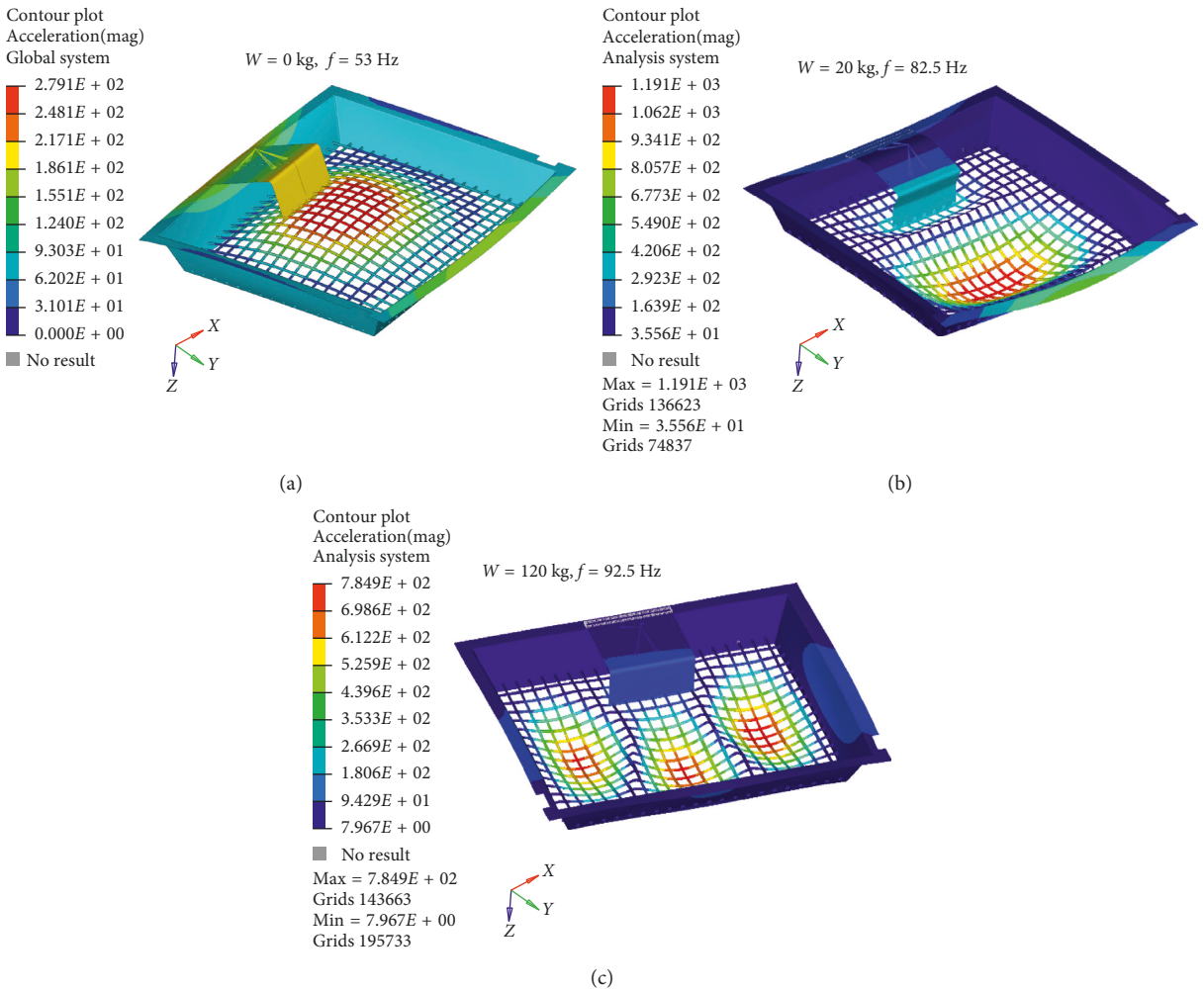

Figure 9: Typical vibrating shapes of the three paths: (a) overall concave of path 1; (b) double concave of path 2; (c) triple concave of path 3.

based on finite element simulations. The detail conclusions can be summed as follows:

(1) The simulation model is strictly built to maximize consistency with the real screen, and the calculated results correspond fairly closely with the testing results. The first three natural frequencies are respectively 25.54, 52.62, 101.57, and 126.29 Hz, and the acceleration of the empty screen center reaches 279 m/s^2 under excitation of 53 Hz.

(2) The load weight has significant influence on the natural frequencies of the screen. All the first four natural frequencies are lowed as the weight increases. Moreover, the modal shape of the fourth frequency also changes when the mass is over 20 kg.

(3) Dynamic response varies dramatically with the change of load weight and excitation frequency. There are three paths that will lead to the sudden increase of vibration acceleration. They are as follows: (1) the load weight variates within 0–50 kg and excitation frequency within 40–60 Hz, and the typical modal shape is overall concave in this region; (2) the load weight variates within 10–100 kg and excitation frequency within 50–90 Hz, and the typical modal shape is double concave; (3) the load weight variates within 80–200 kg and excitation frequency within 70–100 Hz, and the typical modal shape is triple concave.

Abbreviations

Nomenclature

A: Eigenvector
a: Acceleration (m/s^2)
C: Damping
F: Excitation force
f: Frequency (Hertz)
f_e: Excitation frequency (Hertz)
K: Stiffness
M: Mass
t: Time (second)
u: Displacement
W: Weight (kg)
x, y, z: Cartesian rectangular coordinates

Greek symbols

ω: Eigenvalue

Subscripts

i: Arabic numerals.

Data Availability

The data used to support the findings of this study are available from the corresponding author upon request.

Conflicts of Interest

The authors declare that they have no conflicts of interest.

Acknowledgments

This study was funded by the National Natural Science Foundation of China (no. 51705143) and Hunan Provincial Natural Science Foundation of China (nos. 2018JJ3164 and 2017JJ1015).

References

[1] B. Ramatsetse, K. Mpofu, and O. Makinde, "Failure and sensitivity analysis of a reconfigurable vibrating screen using finite element analysis," *Case Studies in Engineering Failure Analysis*, vol. 9, pp. 40–51, 2017.

[2] J. Steyn, "Fatigue failure of deck support beams on a vibrating screen," *International Journal of Pressure Vessels and Piping*, vol. 61, no. 2-3, pp. 315–327, 1995.

[3] Z. Wang, C. Liu, J. Wu, H. Jiang, and Y. Zhao, "Impact of screening coals on screen surface and multi-index optimization for coal cleaning production," *Journal of Cleaner Production*, vol. 187, pp. 562–575, 2018.

[4] L. Peng, H. Jiang, X. Chen et al., "A review on the advanced design techniques and methods of vibrating screen for coal preparation," *Powder Technology*, vol. 347, pp. 136–147, 2019.

[5] Z. Li, X. Tong, B. Zhou, and X. Wang, "Modeling and parameter optimization for the design of vibrating screens," *Minerals Engineering*, vol. 83, pp. 149–155, 2015.

[6] S. A. Zahedi and V. Babitsky, "Modeling of autoresonant control of a parametrically excited screen machine," *Journal of Sound and Vibration*, vol. 380, pp. 78–89, 2016.

[7] Y. Song, X. H. Jiang, J. Song, and J. X. Zhang, "Dynamic analysis of a chaotic vibrating screen," *Procedia Earth and Planetary Science*, vol. 1, no. 1, pp. 1525–1531, 2009.

[8] X. Xiong, L. Niu, C. Gu, and Y. Wang, "Vibration characteristics of an inclined flip-flow screen panel in banana flip-flow screens," *Journal of Sound and Vibration*, vol. 411, pp. 108–128, 2017.

[9] L. Peng, Z. Wang, W. Ma, X. Chen, Y. Zhao, and C. Liu, "Dynamic influence of screening coals on a vibrating screen," *Fuel*, vol. 216, pp. 484–493, 2018.

[10] L. Zhao, Y. Zhao, C. Bao, Q. Hou, and A. Yu, "Optimisation of a circularly vibrating screen based on DEM simulation and Taguchi orthogonal experimental design," *Powder Technology*, vol. 310, pp. 307–317, 2017.

[11] B. B Silva, E. R. Cunha, R. M. Carvalho, and L. M. Tavares, "Modeling and simulation of green iron ore pellet classification in a single deck roller screen using the discrete element method," *Powder Technology*, vol. 332, pp. 359–370, 2018.

[12] G. Wang and X. Tong, "Screening efficiency and screen length of a linear vibrating screen using DEM 3D simulation," *Mining Science and Technology (China)*, vol. 21, no. 3, pp. 451–455, 2011.

[13] A. A. Harzanagh, E. C. Orhan, and S. L. Ergun, "Discrete element modelling of vibrating screens," *Minerals Engineering*, vol. 121, pp. 107–121, 2018.

[14] P. W. Cleary, P. Wilson, and M. D. Sinnott, "Effect of particle cohesion on flow and separation in industrial vibrating screens," *Minerals Engineering*, vol. 119, pp. 191–204, 2018.

[15] Y. M. Zhao, C. S. Liu, X. M. He, C. Y. Zhang, Y. B. Wang, and Z. T. Ren, "Dynamic design theory and application of large vibrating screen," *Procedia Earth and Planetary Science*, vol. 1, pp. 776–784, 2009.

[16] S. Baragetti, "Innovative structural solution for heavy loaded vibrating screens," *Minerals Engineering*, vol. 84, pp. 15–26, 2015.